RSC Advances

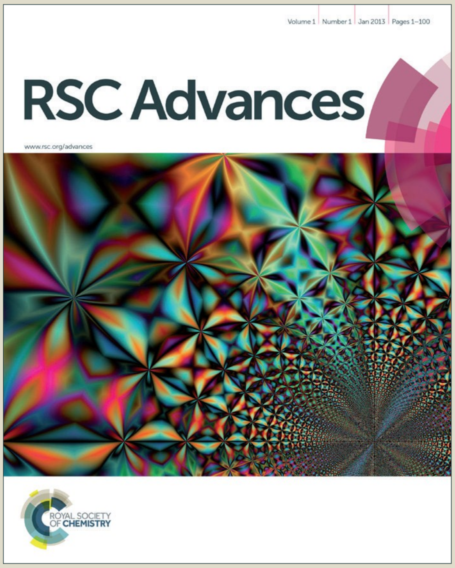

Volume 1 | Number 1 | Jan 2013 | Pages 1–100

RSC Advances

www.rsc.org/advances

ROYAL SOCIETY OF CHEMISTRY

ROYAL SOCIETY OF CHEMISTRY

www.rsc.org/advances

RSC Advances

ARTICLE

Cite this: DOI: 10.1039/x0xx00000x

Axially Phenoxylated Aluminum Phthalocyanines and Their Application in Organic Photovoltaic Cells

*Hasan Raboui[a], Mohammad AL-Amar[a], Ahmed I. Abdelrahman[a] and Timothy P. Bender[a,b,c,]**

Received 00th January 2012,
Accepted 00th January 2012

DOI: 10.1039/x0xx00000x

www.rsc.org/

Novel axially phenoxylated aluminium phthalocyanines, pentafluorophenoxy aluminium phthalocyanine (F_5PhO-AlPc) and *p*-nitrophenoxy aluminium phthalocyanine (NO_2PhO-AlPc), were synthesized through a one-step reaction starting from the commonly used photoactive material, chloro aluminium phthalocyanine (Cl-AlPc), and the respective phenols. Reactions with other phenols did not yield corresponding AlPc derivatives. Optical, electrical, and thermal analyses were carried out on F_5PhO-AlPc and NO_2PhO-AlPc using UV-Vis measurements (solution and thin-film), cyclic voltammetry (CV), differential-pulse voltammetry (DPV), and thermogravimetric analysis (TGA). A simple thermodynamic model was used to explain the lack of reaction when Cl-AlPc was treated with phenol and a variety of alkylated phenols. We noted a side reaction producing fluoro aluminium phthalocyanine (F-AlPc) when the synthesis of F_5PhO-AlPc was attempted in DMF. The model also explains this observation. F_5PhO-AlPc and NO_2PhO-AlPc were integrated into organic photovoltaic devices (OPVs) both as electron-donating and as electron-accepting materials. The phenoxy-AlPcs enable an enhancement of the open-circuit voltage (V_{OC}) of the OPVs when applied as either an electron donor and as an electron acceptor compared to Cl-AlPc. The results within the OPV, specifically the increased V_{OC}, are consistent with the steric shielding effect seen in other OPVs.

Introduction

Phthalocyanines (Pcs) are a family of molecules initially discovered in the early 20th century and have since been industrially produced and used extensively in the pigment industry.[1,2] Pcs possess certain characteristics which enable their use within the pigment industry including high thermal- and photo-stability, ease of synthesis through a one-step reaction (generally) and high molar extinction coefficients. More recently Pcs have demonstrated the ability to move electrical charge and be applied as organic semiconductors in a variety of organic electronic applications including organic photoreceptors,[3-5] organic photovoltaics (OPV)[6-11] and organic light emitting diodes (OLED).[12,13] Pcs have a tight connection to OPVs as one of the first functioning OPVs reported in the literature used copper phthalocyanine (CuPc) as an electron-donor material with a power conversion efficiency (PCE) just under 1%.[14] Since then, many OPV devices have been fabricated using different Pc derivatives whereby Pcs have most commonly been applied as electron donating mateirals[6,15,16] or as light sensitizers.[17-20] Xue *et al* achieved efficiencies up to 5% using Pcs in the light-absorbing layer.[21] There is however limited research on using Pcs as electron acceptor materials in OPVs. Very recently, the group of Jones has demonstrated that Cl-AlPc can function as an electron acceptor material when paired with pentacene in an OPV.[22]

Research into Pcs whereby the intended application is within an OPV has divided into two discreet areas: developing new Pcs through chemical modification[9,23-25] or altering the device fabrication process and/or configuration. Each avenue is generally targeting OPVs with higher photo conversion efficiencies (PCEs).[10,11,26-28] However, achieving better basic characteristics such as enhanced OPV open circuit voltage (V_{OC}) through chemical modification is also highly desirable.

Regarding chemical modification in general, there has been extensive research over past decades looking at the chemistry of Pcs through changing of the central atom,[1] peripheral substitution[29-33] or through axial substitution.[34-38] Nearly all elements in the periodic table (95 elements) have been successfully incorporated into Pcs.[1] Some of the most common central atoms are divalent such as Cu, Zn, and Mg. In these divalent cases, tuning the molecular properties is only possible through peripheral substitution and has been shown to affect the solubility,[29,30] stability,[29] optical properties[31] and electrical properties of the resulting Pcs.[32,33]

Trivalent (e.g. Al) and tetravalent (e.g. Si) metal phthalocyanines (AlPc and SiPc respectively) have the unique ability to form axial bonds with different chemical functionalities that can be potentially used to manipulated or influence the properties of the resulting Pc. However, limited reports are available detailing the chemistry of the axial position of trivalent and tetravalent Pcs and the impact that axial modifications have on the properties of the Pcs. The majority of the reports that are available detail the chemistry of axial substitution of silicon phthalocyanine (SiPc)[34] and boron subphthalocyanine (BsubPc)[35-40] and include μ-oxo[41-44] and polymeric Pc derivatives.[45-47]

Our group has shown the axial substitution of BsubPcs with a pentafluoro phenoxy fragment can alter the frontier orbital energies and change the OPV performance characteristics.[48] We have also recently shown that axial phenoxylation can change an SiPc from being largely electronically inactive to something that has potential as an electron acceptor in a fullerene free OPV.[49] Finally, we have demonstrated that changing the axial chloride of Cl-AlPc to a fluoride (F-AlPc) results in major changes in the fundamental properties of the AlPc including its solid state arrangement.[50]

Beside our recently study of F-AlPc the axial chemistry of AlPc has been relatively understudied. Kraus and Louw,[51] Brasseur *et al*,[52] and Sakai *et al*[53] have shown that silver based reagents can be used to axially phenoxylate AlPcs although in only one case was the yield reported and in no cases was the conversion reported.

In this paper, we outline our independent investigation into the axial phenoxylation of chloro aluminum phthalocyanine (Cl-AlPc) with a specific focus on finding a general, easy, inexpensive and high yielding method for phenoxylation whereby high conversion is achieved. High conversion is desirable to simplify the purification process of the material and to minimize the potentiality of impurities being present within the final materials as they are incorporated into organic electronic devices. The investigation of the resulting derivatives in planar heterojunction (PHJ) organic photovoltaic cells (OPVs) was also undertaken. Despite multiple attempts with variety of phenols, only two derivatives, pentafluorophenoxy aluminum phthalocyanine (F_5PhO-AlPc) and *p*-nitrophenoxy aluminum phthalocyanine (NO_2PhO-AlPc) were successfully synthesized and characterized. Thermodynamic limitations on axial phenoxylation of a range of metal Pcs were calculated. Effects on the optical properties, redox potentials, solid-state packing, and stability were observed. OPVs were fabricated employing F_5PhO-AlPc and NO_2PhO-AlPc both as an electron donor and as an electron acceptor. OPV characteristics were compared against Cl-AlPc baseline devices.

Experimental Section

Materials.

All ACS grade solvents (except nitrobenzene and quinoline) were purchased from Caledon Labs (Caledon, Ontario, Canada) and used without further purification unless otherwise stated. Phthalonitrile were purchased from TCI America (Portland, Oregon, USA) and used as received. Aluminum chloride, *p*-nitrophenol, *m*-cresol, 3-pentadecylphenol, 2-*sec*-butylphenol, 4-*tert*-octylphenol, nitrobenzene, quinoline, decamethyl ferrocene and tetrabutylammonium perchlorate were purchased from Sigma-Aldrich Chemical Company (Mississauga, Ontario, Canada) and used as received. Pentafluoro phenol was purchased from Oakwood Products, Inc. (Columbia, South Carolina, USA) and used as received. Bathocuproine (BCP 99.99%) from Sigma-Aldrich, Ag (99.99%) from R. D. Mathis Company, Fullerene (C_{60}) from SES Research and α-sexithiophene (α-6T) from Sigma-Aldrich were all used as received.

General Methods.

All reactions were performed under an atmosphere of nitrogen gas using oven-dried glassware. Low-resolution mass spectra (LRMS) and high-resolution mass spectra (HRMS) were determined using Waters GC Premier using time-of-flight spectrometer with electron ionization source (TOF-EI MS). X-ray diffraction data were collected on a Bruker Kappa APEX-DUO diffractometer using a Copper ImuS (microsource) tube with multi-layer optics (F_5PhO-AlPc) or a molybdenum sealed tube with Triumph momochromator (NO_2PhO-AlPc) and were measured using a combination of f scans and w scans. The data were processed using APEX2 and SAINT.[54] Absorption corrections were carried out using SADABS.[54] The structure was solved and refined using SHELXT & SHELXL-2103[55] for full-matrix least-squares refinement that was based on F2. Ultraviolet-visible (UV-Vis) absorption spectra were acquired on a PerkinElmer Lambda 1050 UV/VIS/NIR spectrometer using a PerkinElmer quartz cuvette with a 10 mm path length. Cyclic voltammetry and differential-pulse voltammetry were carried out using a Bioanalytical Systems C3 electrochemical workstation. The working electrode was a 1 mm glassy carbon disk, the counter electrode was a platinum wire, and the reference electrode was Ag/AgCl saturated salt solution. Spec-grade solvents were purged with nitrogen gas at room temperature prior to their use. The scanning rate applied throughout both experiments is 100 mV/s. Tetrabutyl ammonium perchlorate (0.1 M) was used as the supporting electrolyte and decamethyl ferrocene as an internal reference. All half-wave potentials were corrected to the half-wave reduction potential ($E_{1/2,red}$) of decamethyl ferrocene. Thermogravimetric analysis was run using TA Instruments Q50 under an atmosphere of nitrogen and a heating rate of 5 °C/ min. Soxhlet extractions were performed using Whatman® single thickness cellulose extraction thimbles.

Synthetic Methods.

Chloro aluminum phthalocyanine (Cl-AlPc) was synthesized as described by Santerre *et al.*[56] 20 g (0.16 mol) of phthalonitrile was added to a solvent-mixture of quinolone (20 mL) and nitrobenzene (32 mL) in a 250-mL round-bottom flask. The solution was cooled to 0 °C in an ice-bath and 5.72 g (0.0439 mol) of $AlCl_3$ was added to the mixture. The reaction was brought up to reflux at 210 °C and left stirring for 4 hours. The resulting blue-greenish solution was cooled to room temperature. The crude product was filtered using a glass-frit filter and washed thoroughly with acetone and acetonitrile. A Soxhlet extraction with acetone was performed overnight on the resulting cake. After the product was dried overnight in the vacuum-oven, 11.2 g (49.9% yield) of blue powder was collected. TOF-EI MS (Figure S1) *m/z* (%): 539.1 [MPc^+] (30), 540.1[MPc^+] (10), 574.1 (100), 575.1 (20). The product was then purified through conventional temperature-gradient train sublimation apparatus (as describe elsewhere[57]). Anal. Calcd for $C_{32}H_{16}N_8AlCl$: C, 66.85; H, 2.81; N, 19.49. Found: C, 66.57; H, 3.38; N, 19.37.

Pentafluorophenoxy Aluminum Phthalocyanine (F_5PhO-AlPc) was synthesized by an adapted method from the synthesis of F_5BsubPc.[58] 1.0 g (1.7 mmol) of Cl-AlPc was mixed with 5 molar excess of pentafluoro phenol (1.7 g) in 20 mL of toluene. The reaction mixture was heated and kept under reflux for 24 hours. After the mixture as allowed to cool down, toluene was removed using rotary evaporation. The powered was then washed successively with toluene. The resulting blue powder was dried in a vacuum oven overnight. 1.2 g (~ 100% yield) of the product was collected. TOF-EI (Figure S2) *m/z* (%): 539.1 [MPc^+] (100), 540.1[MPc^+] (20), 722.1 (100), 723.1 (20). Further purification of the product (0.56 g) took place using the temperature gradient train sublimation apparatus (as describe elsewhere[57]) yielding 49.3% of pure product. TOF-EI MS *m/z* (%): 539.1 [MPc^+] (100), 540.1[MPc^+] (20), 722.1 (100), 723.1 (20). Anal. Calcd for $C_{38}H_{16}N_8AlOF_5$: C, 63.17; H, 2.23; N, 15.51. Found: C, 63.26; H, 2.76; N, 15.59.

***p*-Nitrophenoxy Aluminum Phthalocyanine (NO_2PhO-AlPc)** was ,also, synthesized by an adapted method from the synthesis of F_5BsubPc.[58] 0.5 g (1.35 mmol) of Cl-AlPc was mixed with 5 molar excess of *p*-nitrophenol (0.6 g) in 10 mL of chlorobenzene. The reaction mixture was heated and kept under reflux for 24 hours. After the mixture as allowed to cool down, chlorobenzene was removed using rotary evaporation. The powder was then washed with ethyl ether. The resulting blue powder was dried in a vacuum oven overnight. 0.5 g (84.9% yield) of the product was collected. TOF-EI MS (Figure S4) *m/z* (%): 539.1 [MPc^+] (100), 540.1[MPc^+] (20), 677.2 (50), 678.2 (10). The reaction was also run in DMF producing similar results. The product was then taken into the train sublimation apparatus at 450 °C; the yield of the sublimed product, however, was low (~ 10%). Anal. Calcd for $C_{38}H_{16}N_9AlO_3$: C, 67.36; H, 2.98; N, 18.60. Found: C, 66.78; H, 2.29; N, 18.57.

Device Fabrication.

All OPVs device were fabricated on commercially available patterned ITO substrates (Thin Film Device Inc. (TFD)) with 145 nm ITO thickness and a sheet resistance of 15 Ω/□. The ITO surfaces were ultrasonically cleaned in detergent, distilled water, acetone, methanol, and finally dried in flowing nitrogen. Subsequently, ITO was treated by plasma for 5 min to remove carbon residues. After plasma treatment, a CHEMAT Technology KW-A4 spin coater was used to spin a layer of PEDOT:PSS (Clevios™ P VP AI 4083) at 500 rpm for 10 sec and 4000 rpm for 30 sec on the ITO electrode anode. The ITO with the PEDOT:PSS coating was annealed in a at 110 °C for 15 min. The device structure grown by thermal evaporation with a base pressures of $10x10^{-8}$ torr consists ITO/PEDOT:PSS/Active layer/BCP(8 nm)/Ag(80 nm), where active layer and their thickness can be found in Table 1. Between growth of the BCP layer and the Ag cathode, devices were transferred from the vacuum chamber to nitrogen atmosphere glove box throw a gate, without a vacuum break, to attach a shadow mask consisting 5 active pixel area of 0.2 cm^2 openings then transferred back to the vacuum chamber. Layer thickness and deposition rate were monitored using a quartz crystal microbalance (QCM). After the Ag layer was deposited, the OPV devices were transferred directly from the vacuum chamber back to the nitrogen atmosphere glove box. Silver paste (PELCO® Conductive Silver 187) was applied to the end Ag of electrode and ITO contact point to enhance electrical contact and left to cure for 30 minutes before testing. A 300 W ozone free xenon arc lamp with an air Mass 1.5 Global filter, fed through a Cornerstone™ 260 1/4 m monochromator and then into the glove box by way of a single branch liquid light guide was utilized as a solar simulator. The illumination levels for the test cell were kept at $100mW/cm^2$. A UV-silicon photo-detector was used to calibrate the measurements. The current densities versus voltage (J–V) characteristics and external quantum efficiency were recorded using a Keithley 2401 Low Voltage sourcemeter controlled by a custom LabView program and a Newport Optical Power Meter 2936-R controlled by TracQ Basic software, respectively, in the nitrogen atmosphere glove box.

Results and Discussion

We began this study by surveying the reaction of chloro aluminum phthalocyanine (Cl-AlPc) with a variety of phenols by adopting the simple method our laboratory has used for phenoxylation of chloro boron subphthalocyanine (Cl-BsubPc).[58] This approach is high yielding for BsubPcs and involves nothing more than simple heating in solution with a molar excess of the appropriate phenol. Phenols that we tried included several alkylated phenols (*m*-cresol, 2-sec-butylphenol, 4-*tert*-octylphenol, and 3-pentadecylphenol) and two more 'acidic' phenols (pentafluoro phenol and 4-nitrophenol, **Scheme 1**). Compared against the reaction of Cl-BsubPc, conversion of Cl-

AlPc to the corresponding phenoxylated derivative was low and impractical when alkylated phenols were used. At low molar excesses of alkylated phenol (5 equiv) no conversion of Cl-AlPc was observed. Using large molar excesses (~100-150 equiv) low conversion was at times observed (50% maximum) but was not reproducible. These observations are in line with that of Owen and Kenney.[59] We did not consider the use of the methods described by Kraus and Louw,[51] Brasseur *et al*[52] or Sakai *et al*[53] as all use expensive silver salts to activate the Al-Cl bond to reaction.

The only reproducible syntheses were found to be where the 'acidic' phenols pentafluoro phenol (F_5PhOH) and 4-nitrophenol (NO_2PhOH) were reacted with Cl-AlPc. F_5PhO-AlPc was successfully synthesized using toluene as a solvent and NO_2PhO-AlPc with chlorobenzene. The general workup of the reaction involved rotary evaporating the crude solution to dryness. The powder was then washed with an appropriate organic solvent and dried in a vacuum-oven overnight. Both F_5PhOH and NO_2PhOH produced high yields (>80%) of the respective AlPc derivatives. Each product was then purified by train sublimation.[57]

The identity of each phenoxylated AlPc was first confirmed using LR-MS and HR-MS (Figure Conversely, we were able to obtain single crystals of NO_2PhO-AlPc grown by sublimation an analogous process to that which is used for fabrication of OPV devices (Figures S5-S6, Table S7-S12, CCDC deposition #1052023). It was found that the solid-state packing of NO_2PhO-AlPc is extremely dense (Figure S6) with π-π interactions between the AlPc chromaphores at distances less than 3.8 Å in all three crystallographic axis; a desirable characteristic for an organic electronic material. The obvious point of comparison would be the solid-state arrangement of Cl-AlPc. While there is a crystal structure of Cl-AlPc report by Wynne,[42] as noted there is significant disorder within the unit cell of the single crystal. The absolute positions of two Cl-AlPc molecules were determined but the position(s) of the remaining one or two molecules could not be determined.[42] Therefore without a point of comparison, a more in depth discussion of the solid-state arrangement of NO_2PhO-AlPc is irrelevant. We have made several attempts in our laboratory to obtain single crystals of Cl-AlPc without success.

Determination of the NMR spectra for both F_5PhO-AlPc and NO_2PhO-AlPc was not possible due to their limited solubility (common for Pcs). While each did have limited solubility in DMSO, DCM and toluene each had only enough solubility in DMSO to yield an NMR spectrum. NMR analysis in DSMO-d_6 showed that each reacted with residual water to produce the same hydrolyzed product (presumably HO-AlPc). Final purity of each material was therefore confirmed using elemental analysis (see experimental) prior to OPV device integration.

Given the polarity of the acidic phenols, we also tried the corresponding reactions in DMF. However, in DMF the reaction of pentafluoro phenol and Cl-AlPc yielded exclusively F-AlPc as confirmed by MS (Figure S7). Shoute *et al.* has studied the defluoration of pentafluoro phenol and formation of fluoride ions in aqueous solutions.[60] We hypothesize that the residual water present in reagent grade DMF (and not in reagent grade toluene) allowed for the generation of fluoride ions and their subsequent reaction with Cl-AlPc to produce F-AlPc. NO_2PhO-AlPc could also be synthesized in toluene or DMF as well as chlorobenzene as the solvent without issue.

Thermodynamic Limitations.

As outlined above, only two out of the six phenols successfully formed phenoxylated AlPcs whereas multiple examples of phenoxylation of SiPcs[34,49] and BsubPcs[35-40] using a similar processes are known. In an effort to explain these observations, we turned to an estimation of the enthalpy of the phenoxylation reaction (ΔH_R) for different MPcs. The phenoxylation reaction was assumed to follow Scheme 1 and we have made no assumptions regarding the mechanism by which the reaction occurs. ΔH_R was simply estimated using bond dissociation enthalpies of the bonds involved in the phenoxylation reaction for several MPcs (Equation 1). To a first approximation, ΔH_R is assumed to depend only on the bonds being broken and formed during the reaction and not being dependent on the molecule as a whole.[61]

$$\Delta H_R = (\Delta H_{H-X} + \Delta H_{O-M}) - (\Delta H_{X-M} + \Delta H_{O-H}) \qquad \text{Equation 1}$$

ΔH_{A-B} is the enthalpy of formation of the bond between A and B. If we assume that the entropy of the products and the reactants are similar and that the changes in entropy can be neglected (since the number of moles throughout the reaction is constant and since the reaction is run in solution without a phase change) then the sign and magnitude of ΔH_R can indicate whether the reaction will proceed to completion spontaneously or not.

As can be seen in Figure 1, using our simple model the phenoxylation of Cl-AlPc does not seem to be thermodynamically favorable since the value of ΔH_R is estimated to be approximately zero. The value for Br-AlPc is negative and for F-AlPc positive indicating that a phenoxylation reaction on Br-AlPc might be favorable whereas reaction on F-AlPc would not be favorable. It also means that in the presence of fluoride anions the formation of F-AlPc from Cl-AlPc is more thermodynamically favorable than formation of the phenoxylated AlPc. This supports the observed formation of F-AlPc when pentafluoro phenol was used in DMF. Using this simple model the reaction of X-SiPc and X-BsubPc (X = F, Cl, Br) have extremely negative ΔH_R values and is therefore consistent with the ease by which each can be phenoxylated and further validates this simple model.

While this basic model explains most of the observations when attempting to phenoxylate Cl-AlPc, the synthesis of F_5PhO-

AlPc and NO_2PhO-AlPc did work. Given the ΔH_R for phenoxylation of Cl-AlPc with each of these 'acidic' phenols is calculated to be near 0, subtle differences in the $\Delta H_{O\text{-}H}$ and $\Delta H_{O\text{-}M}$ values may cause a change in the sign of ΔH_R and, hence, the spontaneity of the reaction. Subtle differences could be attributable to the acid dissociation constants (pK_a); F_5PhOH and NO_2PhOH are 5.5[60] and 7.15[62], respectively, compared to pK_a's over 10 for alkylated phenols.[62]

Properties of Phenoxy-AlPcs.

Optical absorption measurements were taken for Cl-AlPc, NO_2PhO-AlPc, and F_5PhO-AlPc (Figure 2). Minimal differences between the three compounds were observed. F_5PhO-AlPc shows maximum absorption at λ_{max}= 676 nm while Cl-AlPc and NO_2PhO-AlPc have λ_{max}= 680 and λ_{max}= 678, respectively (DMSO solution). Solid-state absorbance spectra were taken from vacuum-deposited thin-films (~1000 nm thick). The solid-state spectra were broader with peak absorptions slightly red-shifted from the solution spectra. Optical band gabs (E_{OG}) were calculated using the onset of the main absorption peak. The differences in E_{OG} between the three compounds were insignificant, with E_{OG} ranging between 1.40-1.55 eV.

Electrochemical oxidation and reduction potentials were measured using cyclic voltammetry (CV) and differential-pulse voltammetry (DPV) and are again consistent within this series of compounds (Figure 3). Estimations of HOMO and LUMO levels were calculated using the empirical model developed by Dandrade *et al.*[63] and the oxidation and reduction peaks from the DPV data (Table 1). Electrochemical energy gap (E_{EG}) was defined and calculated as the difference between the oxidation and reduction peaks of the DPV data. The calculated values of NO_2PhO-AlPc, and F_5PhO-AlPc are nearly the same as the energy levels of Cl-AlPc that are found in the literature.[64]

The thermal stability of all AlPc derivatives was measured using thermogravimetric analysis (TGA, Figure 4). All of the three compounds showed two mass losses. Both phenoxylated AlPcs have a drop in mass at a lower temperature than the Cl-AlPc, between 350 °C and 400 °C compared to ~500 °C for Cl-AlPc. The amount of mass lost corresponds approximately to the mass of the axial phenoxy groups and is therefore probably attributable to the detachment of the axial functionality. This analysis establishes the temperature window for device integration by vacuum deposition.

Device Integration.

Multiple organic photovoltaic (OPV) devices were fabricated using Cl-AlPc, F_5PhO-AlPc, and NO_2PhO-AlPc as both an electron donor and as an electron acceptor material paired with either C_{60} or sexithiophene (α6T), respectively. C_{60} is a well-known electron acceptor material and α6-T is a well-known electron donor material. The application of each has been well documented in many OPV device structures.[65-67] Cl-AlPc is also a relatively well studied organic semiconductor material that has been used as both an electron donor[64,68] and an electron acceptor[22] material within OPVs, therefore is a good comparison point.

To begin, and as a point of comparison, we constructed baseline OPVs with active layer configurations of Cl-AlPc(20 nm)/C_{60}(40 nm) and α6T (60 nm)/Cl-AlPc(20 nm). For Cl-AlPc(20 nm)/C_{60}(40 nm) OPV the current short circuit density (J_{SC}) was measured at 3.85 mA/cm^2, the open circuit voltage (V_{OC}) at 0.67 V and the fill factor (FF) at 0.48 for an overall efficiency (η) of 1.23%. This is in line with the cell characteristics reported in the literature.[64, 68-71] For the α6T (60 nm)/Cl-AlPc(20 nm) cell the J_{SC} was 3.82 mA/cm^2, V_{OC} was 0.61 V, FF 0.44 for an η of 1.02%. No point of comparison is available for the α6T/Cl-AlPc cell in the literature. The results are tabulated in Table 2 and the corresponding J-V and EQE plots are illustrated in Figures 5 and 6.

Moving to the phenoxylated derivatives as electron donating materials, for the F_5PhO-AlPc(20 nm)/C_{60}(40 nm) and NO_2PhO-AlPc(20 nm)C_{60}(40 nm) OPVs, the J_{SC} values were 2.92 and 2.63 mA/cm^2, V_{OC} values were 0.80 V and 0.82 V, FF values were 0.44 and 0.40 for overall η of 1.06 % and 0.86 %, respectively. When results are compared against the baseline Cl-AlPc(20 nm)/C_{60}(40 nm), the OPVs containing the phenoxylated derivatives had a V_{OC} for the F_5PhO-AlPc/C_{60} device 130 mV larger than for the Cl-AlPc/C_{60} device however, the J_{SC} was 0.88 mA/cm^2 smaller. The same general observations were seen for the NO_2PhO-AlPc/C_{60} OPV with a V_{OC} 132 mV larger than for Cl-AlPc/C_{60} and again a J_{SC} 1.22 mA/cm^2 lower than that of the Cl-AlPc/C_{60} OPV. The electrical characteristics illustrated in Figure 5 and tabulated in Table 2.

Considering the application of F_5PhO-AlPc, and NO_2PhO-AlPc as electron accepting materials paired with α6T, the following OPVs were constructed: α6T(60 nm)/F_5PhO-AlPc(20 nm) and α6-T(60 nm)/NO_2PhO-AlPc(20 nm). The cells J_{SC} values were 4.2 mA/cm^2 and 2.75 mA/cm^2, V_{OC} values were 0.67 V and 0.66 V and FF values were 0.40 and 0.47 resulting in an overall η of 1.12 % and 0.84 %, respectively (Table 2, Figure 6). Notable, when F_5PhO-AlPc and NO_2PhO-AlPc used as electron acceptors and in line with their application as electron donating materials, an increase in V_{OC} of 50-60 mV over α6T/Cl-AlPc was observed. The J_{SC} of α6T/F_5PhO-AlPc is 0.68 mA/cm^2 larger than that of α6T/Cl-AlPc, however, the J_{SC} of α6-T/NO_2Pho-AlPc is 1.02 mA/cm^2 smaller than that α6T/Cl-AlPc.

Based on the electrical characterization the following conclusions can be made regarding the application of phenoxylated AlPcs in OPVs. All of the AlPcs proved functional both as electron-donating and as electron-accepting materials in an OPV, therefore they are dually functional. There is an observed and consistent increase in V_{OC} for the resulting OPVs when the phenoxylated AlPcs are used in place of Cl-AlPc and with one exception (α6T/F_5PhO-AlPc) the J_{SC} is lower.

These observations are in line with the 'steric shielding effect' described in both polymer[72] and small molecule based OPVs.[73,74] While this effect has been debated[75] the concept is that addition of sterically bulky groups out of plane to the semiconducting π-electron system of an organic material enhances the V_{OC} within an OPV. The V_{OC} enhancement is attributed to the steric bulk increasing the distance between the electron donating and electron accepting materials at their interface thus resulting in a hole-electron pair having more potential. The high potential makes the separation into a hole-electron pair more difficult and therefore OPVs typically see a net drop in J_{SC}.[73]

The results of the integration of the phenoxylated AlPc seem to add positively to the idea of the steric shielding effect. However, to positively state such a conclusion, further device optimization is being undertaken with an aim to improve the FF of the OPVs and to confirm that the reduced J_{SC} (and overall efficiencies) cannot be overcome with more device engineering. Given our electrochemical data does indicate that there are energy differences in the HOMO and LUMO of Cl-AlPc, F_5PhO-AlPc and NO_2PhO-AlPc this could also be contributing to the differences seen in the V_{OC}. Experiments will be undertaken in an effort to separate the relative contributions to the observed V_{OC} differences.

Conclusions

We were successful in phenoxylating Cl-AlPc using pentafluoro phenol and *p*-nitrophenol to produce F_5PhO-AlPc and NO_2PhO-AlPc, respectively. A basic thermodynamic model was developed to explain limitations on conversion of the phenoxylation reaction when alkylated phenols are used. The optical, electrical, and thermal characteristics of the two novel AlPcs were determined. F_5PhO-AlPc and NO_2PhO-AlPcs were applied in OPVs both as electron donors and as electron acceptors paired with C_{60} and α6T respectively. When applied as electron donating materials an increase in the V_{OC} of the OPV of ~130 mV was observed and ~50-60 mV when F_5PhO-AlPc and NO_2PhO-AlPc were applied as electron accepting materials. Given the increase in V_{OC} these novel phenoxylated AlPcs show promise for application within OPVs although further device optimization and engineering is required to enhance the FF and J_{SC} of the OPVs.

Acknowledgements

The authors would like to acknowledge financial support from Saudi Basic Industries (SABIC).

Notes

[a] University of Toronto, Dept. of Chemical Engineering & Applied Chemistry. 200 College Street, Toronto, Ontario M5S 3E5.

[b] University of Toronto, Dept. of Materials Science and Engineering.

200 College Street, Toronto, Ontario M5S 3E5.

[c] University of Toronto, Dept. of Chemistry.

80 St. George Street, Toronto, Ontario M5S 3H6.

* to whom correspondences should be addressed. E-mail: tim.bender@utoronto.ca

Electronic Supplementary Information (ESI) available: High and low resolution mass spectra and crystallographic data. See DOI: 10.1039/b000000x/

References

1. N. B. McKeown, *Phthalocyanine materials : synthesis, structure, and function*, Cambridge University Press, Cambridge ; New York, 1998.
2. F. H. Moser and A. L. Thomas, *Phthalocyanine compounds*, Reinhold Pub. Co., New York, 1963.
3. X. Zhang, Y. Wang, Y. Ma, Y. Ye, Y. Wang and K. Wu, *Langmuir*, 2005, 22, 344-348.
4. L. Cao, H. Chen, M. Wang, J. Sun, X. Zhang and F. Kong,. *B*, 2002, 106, 8971-8975. *J. Phys. Chem*
5. Y. Wang and D. Liang, *Adv. Mater.*, 2010, 22, 1521-1525.
6. G. Williams, S. Sutty, R. Klenkler and H. Aziz, *Sol. Energy Mater. Sol. Cells*, 2014, 124, 217-226.
7. T. Jägeler-Hoheisel, F. Selzer, M. Riede and K. Leo, *J. Phys. Chem. C*, 2014, 118, 15128-15135.
8. W. Li, H. Yu, J. Zhang, Y. Yao, C. Wu and X. Hou, *J. Phys. Chem. C*, 2014, 118, 11928-11934.
9. H. Fukui, S. Nakano, T. Uno, Q.-D. Dao, T. Saito, A. Fujii, Y. Shimizu and M. Ozaki, *Org. Electron.*, 2014, 15, 1189-1196.
10. K. V. Chauhan, P. Sullivan, J. L. Yang and T. S. Jones, *J. Mater. Chem.*, 2010, 6, 1173-1178
11. B. P. Rand, D. Cheyns, K. Vasseur, N. C. Giebink, S. Mothy, Y. Yi, V. Coropceanu, D. Beljonne, J. Cornil, J. L. Brédas and J. Genoe, *Adv. Funct. Mater.*, 2012, 22, 2987-2995.
12. Z. Deng, Z. Lü, Y. Chen, Y. Yin, Y. Zou, J. Xiao and Y. Wang, *Solid-State Electron.*, 2013, 89, 22-25.
13. K. Narayan, S. Varadharajaperumal, G. Mohan Rao, M. Manoj Varma and T. Srinivas, *Curr. Appl Phys.*, 2013, 13, 18-25.
14. C. W. Tang, *Appl. Phys. Lett.*, 1986, 48, 183-185.
15. N. M. Bamsey, A. P. Yuen, A.-M. Hor, R. Klenkler, J. S. Preston and R. O. Loutfy, *Sol. Energy Mater. Sol. Cells*, 2011, 95, 1970-1973.
16. N. Beaumont, I. Hancox, P. Sullivan, R. A. Hatton and T. S. Jones, *Energy Environ. Sci.*, 2011, 5, 1708-1711.
17. D. K. Panda, F. S. Goodson, S. Ray and S. Saha, *Chem. Commun.*, 2014, 50, 5358-5360.
18. A. Hagfeldt, G. Boschloo, L. Sun, L. Kloo and H. Pettersson, *Chem. Rev.*, 2010, 110, 6595-6663.
19. M.-E. Ragoussi, J.-H. Yum, A. K. Chandiran, M. Ince, G. de la Torre, M. Grätzel, M. K. Nazeeruddin and T. Torres, *ChemPhysChem*, 2014, 15, 1033-1036.
20. M.-E. Ragoussi, M. Ince and T. Torres, *Eur. J. Org. Chem.*, 2013, 2013, 6475-6489.
21. J. Xue, B. P. Rand, S. Uchida and S. R. Forrest, *Adv. Mater.*, 2005, 17, 66-71.

22. N. L. Beaumont, Doctor of Philosophy, University of Warwick, 2013.
23. P. Sullivan, A. Duraud, l. Hancox, N. Beaumont, G. Mirri, J. H. R. Tucker, R. A. Hatton, M. Shipman and T. S. Jones, *Adv. Energy Mater.*, 2011, 1, 352-355.
24. S. Schumann, R. A. Hatton and T. S. Jones, *J. Phys. Chem. C*, 2011, 115, 4916-4921.
25. M. V. Martinez-Diaz, G. de la Torre and T. Torres, *Chem. Commun.*, 2010, 46, 7090-7108.
26. S. W. Cho, A. DeMasi, A. R. H. Preston, K. E. Smith, L. F. J. Piper, K. V. Chauhan and T. S. Jones, *Appl. Phys. Lett.*, 2012, 100.
27. I. Hancox, P. Sullivan, K. V. Chauhan, N. Beaumont, L. A. Rochford, R. A. Hatton and T. S. Jones, *Org. Electron.*, 2010, 11, 2019-2025.
28. K. Vasseur, K. Broch, A. L. Ayzner, B. P. Rand, D. Cheyns, C. Frank, F. Schreiber, M. F. Toney, L. Froyen and P. Heremans, *ACS Appl. Mater. Interfaces*, 2013, 5, 8505-8515.
29. E. R. L. Brisson, A. S. Paton, G. E. Morse and T. P. Bender, *Ind. Eng. Chem. Res.*, 2011, 50, 10910-10917.
30. G. Löbbert, in *Ullmann's Encyclopedia of Industrial Chemistry*, Wiley-VCH Verlag GmbH & Co. KGaA, 2000, DOI: 10.1002/14356007.a20_213.
31. S. M. O'Flaherty, S. V. Hold, M. J. Cook, T. Torres, Y. Chen, M. Hanack and W. J. Blau, *Adv. Mater.*, 2003, 15, 19-32.
32. B. A. Kamino and T. P. Bender, *Dalton Trans.*, 2013, 42, 13145-13150.
33. G. E. Morse, M. G. Helander, J. Stanwick, J. M. Sauks, A. S. Paton, Z.-H. Lu and T. P. Bender, *J. Phys. Chem. C*, 2011, 115, 11709-11718.
34. C. A. Barker, K. S. Findlay, S. Bettington, A. S. Batsanov, I. F. Perepichka, M. R. Bryce and A. Beeby, *Tetrahedron*, 2006, 62, 9433-9439.
35. J. Guilleme, L. Martínez-Fernandez, D. Gonzalez-Rodríguez, I. Corral, M. Yáñez and T. Torres, *Journal of American Chemical Society*, 2014, 136, 14289-14298.

36. M. V. Fulford, D. Jaidka, A. S. Paton, G. E. Morse, E. R. L. Brisson, A. J. Lough and T. P. Bender, *J. Chem. Eng. Data*, 2012, 57, 2756-2765.
37. G. E. Morse, J. S. Castrucci, M. G. Helander, Z.-H. Lu and T. P. Bender, *ACS Appl. Mater. Interfaces*, 2011, 3, 3538-3544.
38. A. S. Paton, G. E. Morse, A. J. Lough and T. P. Bender, *CrystEngComm*, 2011, 13, 914-919.
39. A. S. Paton, G. E. Morse, D. Castelino and T. P. Bender, *J. Org. Chem.*, 2012, 77, 2531-2536.
40. J. Guilleme, D. González-Rodríguez and T. Torres, *Angew. Chem. Int Ed.*, 2011, 50, 3506-3509.
41. K. J. Wynne, *Inorg. Chem.*, 1985, 24, 1339-1343.
42. K. J. Wynne, *Inorg. Chem.*, 1984, 23, 4658-4663.
43. M. V. Fulford, A. J. Lough and T. P. Bender, *Acta Crystallogr., Sect. B: Struct. Sci.*, 2012, 68, 636-645.
44. Y. Yamasaki and K. Takaki, *Dyes Pigm.*, 2006, 70, 105-109.
45. P. Samorí, H. Engelkamp, P. A. J. de Witte, A. E. Rowan, R. J. M. Nolte and J. P. Rabe, *Adv. Mater.*, 17, 1265-1268.
46. A. de la Escosura, M. V. Martínez-Díaz, T. Torres, R. H. Grubbs, D. M. Guldi, H. Neugebauer, C. Winder, M. Drees and N. S. Sariciftci, *Chem. - Asian J.*, 2006, 1, 148-154.
47. N. B. McKeown, *J. Mater. Chem.*, 2000, 10, 1979-1995.
48. G. E. Morse, J. L. Gantz, K. X. Steirer, N. R. Armstrong and T. P. Bender, *ACS Appl. Mater. Interfaces*, 2014, 6, 1515-1524.
49. B. H. Lessard, R. T. White, M. AL-Amar, T. Plint, J. S. Castrucci, D. S. Josey, Z.-H. Lu and T. P. Bender, *ACS Appl. Mater. Interfaces,* 2015, DOI: 10.1021/am508491v.
50. B. H. Lessard, M. AL-Amar, T. M. Grant, R. White, Z.-H. Lu and T. P. Bender, *J. Mater. Chem. A*, 2015, 3, 5047-5053.
51. G. A. Kraus and S. J. V. Louw, *Synlett*, 1996, 1996, 726-726.
52. N. Brasseur, R. Ouellet, C. L. Madeleine and J. E. v. Lier, *Br. J. Cancer*, 1999, 80, 1533-1541.
53. Y. Sakai, M. Ueda, A. Yahagi and N. Tanno, *Polymer*, 2002, 43, 3497-3503.
54. Bruker, APEX2, SAINT & SADABS, Bruker AXS Inc., Madison, Wisconsin, USA, 2007.
55. G. Sheldrick, *Acta Crystallogr., Sect. A*, 2008, 64, 112-122.
56. F. Santerre, R. Côté, G. Veilleux, R. G. Saint-Jacques and J. P. Dodelet, *J. Phys. Chem.*, 1996, 100, 7632-7645.
57. H. Wagner, R. Loutfy and C.-K. Hsiao, *J. Mater. Sci.*, 1982, 17, 2781-2791.
58. G. E. Morse, M. G. Helander, J. F. Maka, Z.-H. Lu and T. P. Bender, *ACS Appl. Mater. Interfaces*, 2010, 2, 1934-1944.
59. J. E. Owen and M. E. Kenney, *Inorg. Chem.*, 1962, 1, 331-333.
60. L. C. T. Shoute, J. P. Mittal and P. Neta, *J. Phys. Chem.*, 1996, 100, 3016-3019.
61. Y.-R. Luo and J.-P. Cheng, Bond Dissociation Energies, *Handbook of Chemistry and Physics*, 2012 edn., pp. 9-65.
62. Dissociation Constants of Organic Acids and Bases, *Handbook of Chemistry and Physics*, 2014 edn., pp. 5-94.
63. B. Dandrade, S. Datta, S. Forrest, P. Djurovich, E. Polikarpov and M. Thompson, *Org. Electron.*, 2005, 6, 11-20.
64. D. Y. Kim, F. So and Y. Gao, *Sol. Energy Mater. Sol. Cells*, 2009, 93, 1688-1691.
65. C.-Z. Li, H.-L. Yip and A. K. Y. Jen, *J. Mater. Chem.*, 2012, 22, 4161-4177.
66. Y. He and Y. Li, *Phys. Chem. Chem. Phys.*, 2011, 13, 1970-1983.
67. K. Cnops, B. P. Rand, D. Cheyns, B. Verreet, M. A. Empl and P. Heremans, *Nat. Commun.*, 2014, 5, 3406.
68. R. F. Bailey-Salzman, B. P. Rand and S. R. Forrest, *Appl. Phys. Lett.*, 2007, 91, -.
69. V. Chauhan, R. Hatton, P. Sullivan, T. Jones, S. W. Cho, L. Piper, A. deMasi and K. Smith, *J. Mater. Chem.*, 2010, 20, 1173-1178.
70. N. Beaumont, S. W. Cho, P. Sullivan, D. Newby, K. E. Smith and T. S. Jones, *Adv. Funct. Mater.* 2012, 22, 561-566.
71. I. Hancox, K. V. Chauhan, P. Sullivan, R. A. Hatton, A. Moshar, C. P. A. Mulcahy and T. S. Jones, *Energy Environ. Sci.*, 2010, 3, 107-110.
72. L. Yang, H Zhou and W.You, *J. Phys. Chem. C*, 2010, 114, 16793–16800.
73. P. Erwin and M.E. Thompson, *Appl. Phys. Let.*, 2011, 98, 223305.
74. S.L. Lam, Z. Liu, F. Zhao, C.-L. K Less and W.L. Kwan, *Chem. Commun.*, 2013, 49, 4543.

75. K.R. Graham, P. Ewan, D. Nordland, K. Vandewal, R. Li, G.O. Ngongang, E.T. Hoke, A. Salleo, M.E. Thompson, M.D. McGehee and A. Amassian, *Adv. Mater.*, 2013, 25, 6076–6082.

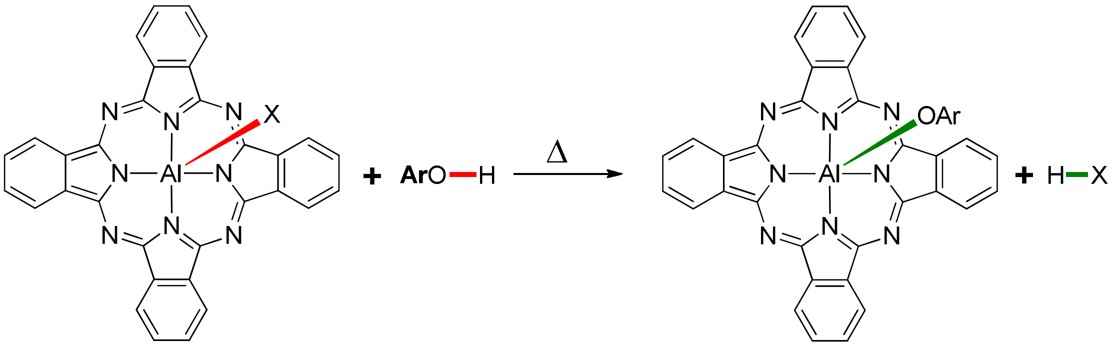

Ar =	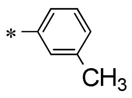	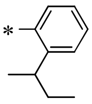	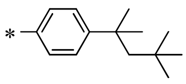	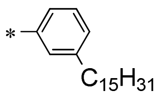	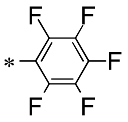	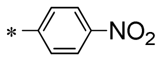
Designation	N/a	N/a	N/a	N/a	F$_5$PhO-AlPc	NO$_2$PhO-AlPc

Scheme 1. Phenoxylation reactions of Cl-AlPc. Where the process did not reproducibly produce a phenoxylated AlPc, a N/a is placed in the designation cell. Changing bonds are highlighted in red and green.

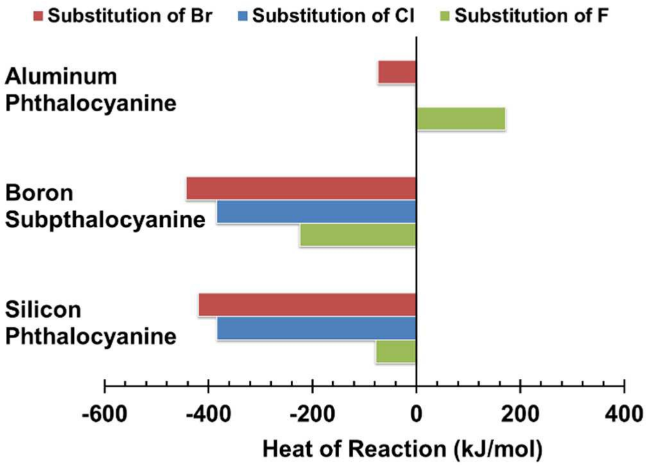

Figure 1. Heat of phenoxylation reaction (ΔH_R) of different halide-MPcs.

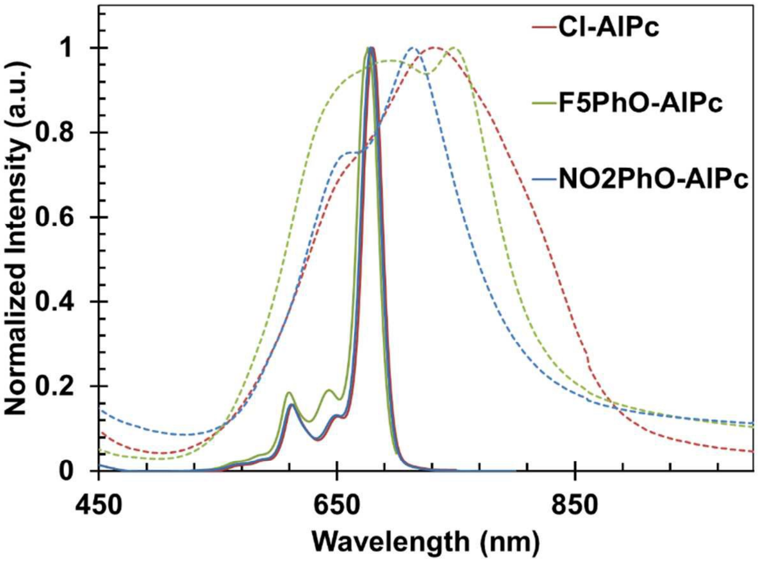

Figure 2. UV-Vis absorption spectra, solution in DMSO (solid line) and solid-state (dashed line), of Cl-AlPc, NO_2PhO-AlPc, and F_5PhO-AlPc.

Table 1. Oxidation and reduction potentials using CV and DPV (in dichloromethane), electrical band gap (E_{EG}), optical band gap (E_{OG}), and the estimated frontier energy levels of AlPc derivatives.

	E_{ox}(V)	E_{red}(V)	E_{EG}(eV)	E_{OG}(eV)	HOMO (eV)	LUMO (eV)
Cl-AlPc	-	-		1.40	5.3[59]	4.0[59]
F_5PhO-AlPc	0.70	-0.71	1.70	1.51	5.52	3.83
NO_2PhO-AlPc	0.60	-0.72	1.58	1.55	5.40	3.82

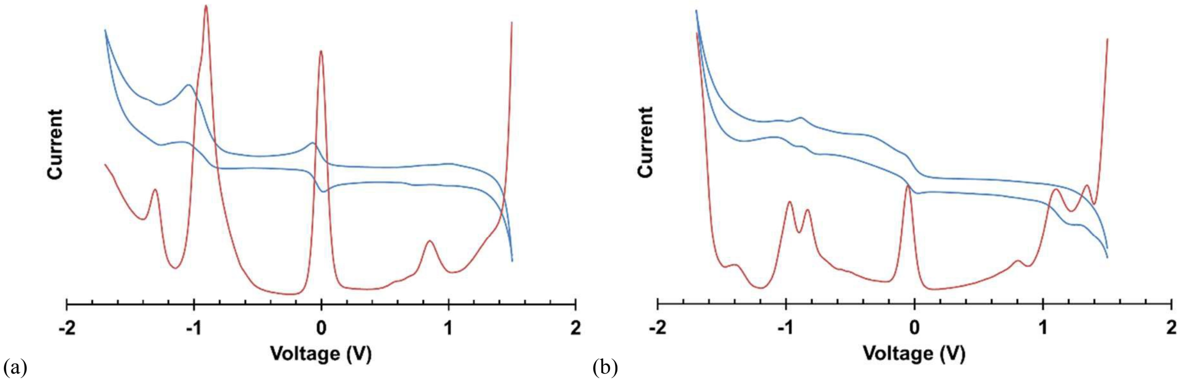

Figure 3. Cyclic voltammetry (blue) and differential-pulse voltammetry (red) of (a) F_5PhO-AlPc and (b) NO_2PhO-AlPc (right).

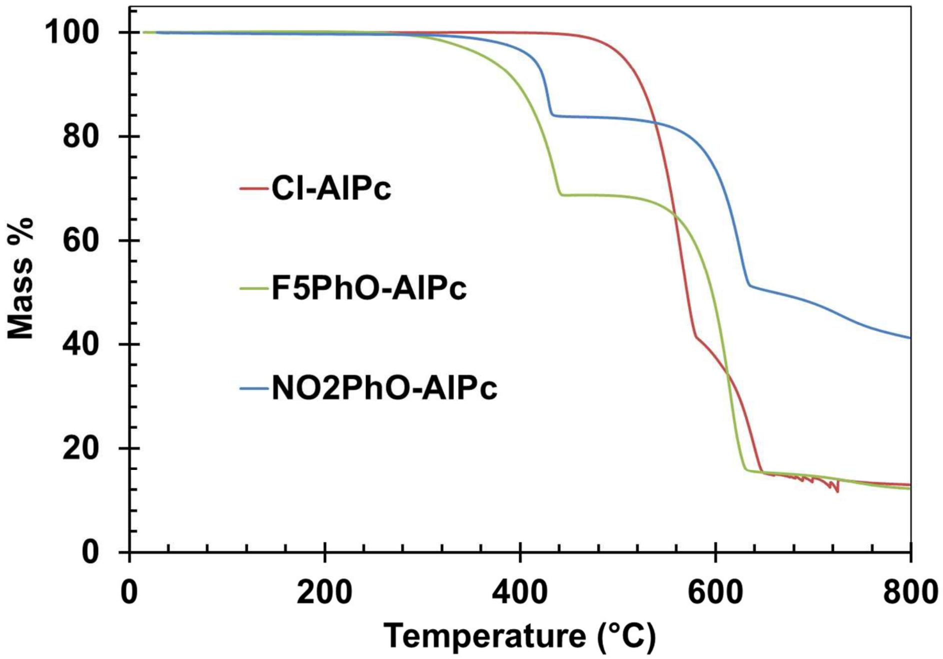

Figure 4. Thermogravimetric analysis (TGA) of Cl-AlPc, F_5PhO-AlPc, and NO_2PhO-AlP.

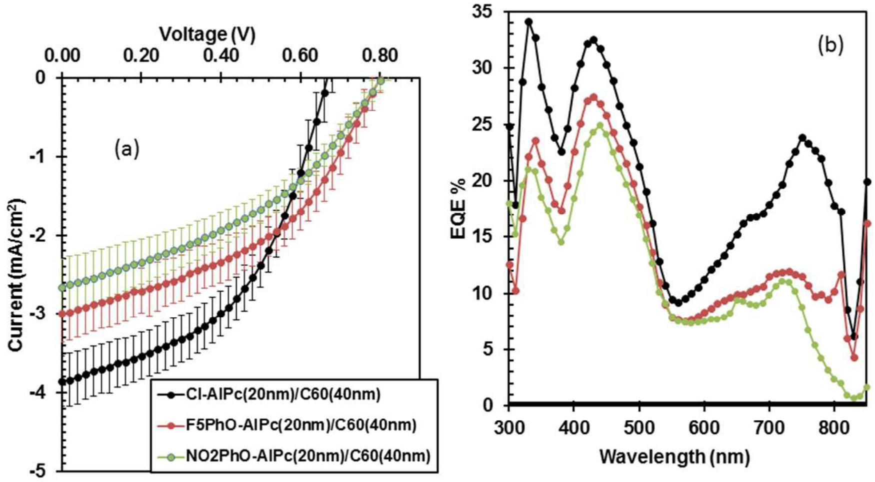

Figure 5. (a) The average J-V curves and **(b)** the average external quantum efficiencies of Cl-AlPc /C_{60}, F_5PhO-AlPc/C_{60}, and NO_2PhO-AlPc/C_{60} OPVs.

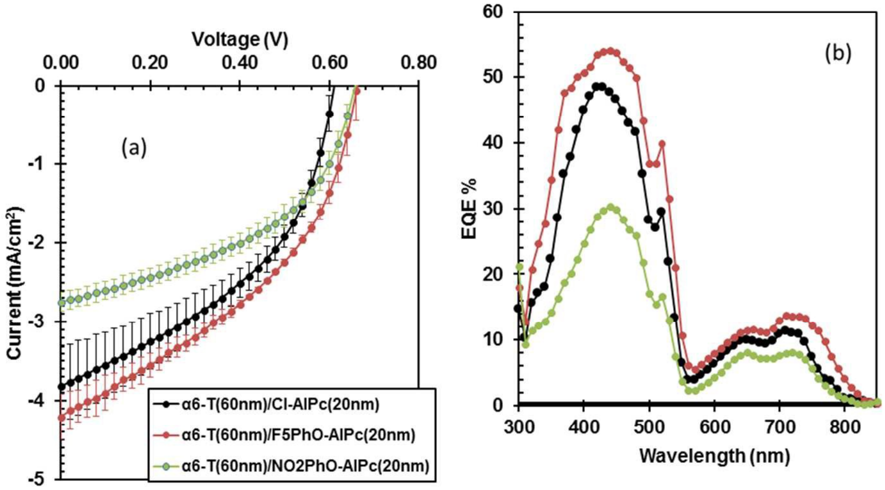

Figure 6. (a) The average J-V curves and **(b)** the average external quantum efficiencies of α-6T/Cl-AlPc, and α-6T/F_5PhO-AlPc, and α-6T/NO_2PhO-AlPc OPVs.

Table 2. The electrical performance and standard deviation of Cl-AlPc /C_{60}, F_5PhO-AlPc /C_{60}, NO_2PhO-AlPc/C_{60}, α-6T/Cl-AlPc, α-6T/F_5PhO-AlPc, and α-6T/NO_2PhO-AlPc OPVs.

Device Structure	$V_{OC}(V)$	$J_{SC}(mA/cm^2)$	*FF*	η *(%)*
Cl-AlPc (20nm)/C_{60} (40nm)	0.67±0.03	-3.85±0.3	0.48±0.03	1.23±0.17
F_5PhO-AlPc (20nm)/C_{60} (40nm)	0.8±0.01	-2.97±0.35	0.44±0.01	1.06±0.14
NO_2PhO-AlPc(20nm)C_{60} (40nm)	0.82±0.01	-2.63±0.38	0.40±0.01	0.86±0.08
α-6T(60nm)/Cl-AlPc(20nm)	0.61±0.009	-3.82±0.5	0.44±0.03	1.02±0.07
α-6T(60nm)/F_5PhO-AlPc(20nm)	0.67±0.007	-4.2±0.3	0.40±0.02	1.12±0.03
α-6T(60nm)/NO_2PhO-AlPc(20nm)	0.66±0.007	-2.75±0.12	0.47±0.02	0.84±0.07

TOC contents.

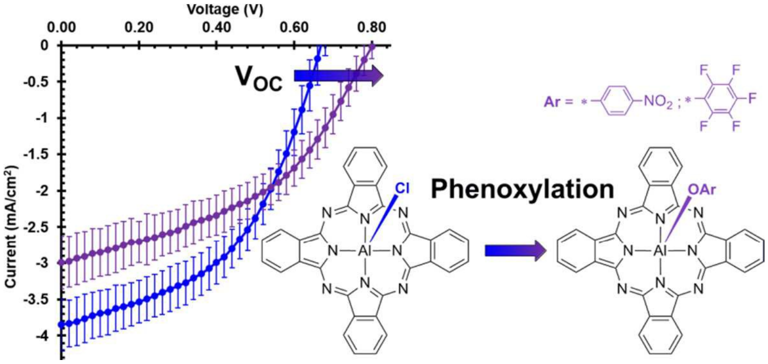

Phenoxylation of chloro aluminum phthalocyanine (Cl-AlPc) can be easily achieved only when using "acidic phenols". Once incorporated into unoptimized organic photovoltaics (OPVs) the result is an increase in the V_{OC}.